Geosciences **2015**, *5*, 222-242; doi:10.3390/geosciences5030222

OPEN ACCESS

geosciences

ISSN 2076-3263

www.mdpi.com/journal/geosciences

Article

Petrologic and Minerochemical Trends of Acapulcoites, Winonaites and Lodranites: New Evidence from Image Analysis and EMPA Investigations †

Vanni Moggi Cecchi [1,‡,*] and Stefano Caporali [2,3,‡]

[1] Dipartimento di Scienze della Terra, Università degli Studi di Firenze, Via La Pira 4, 50121 Florence, Italy

[2] Dipartimento di Chimica, Università degli Studi di Firenze, Via della Lastruccia 3, 50019 Sesto Fiorentino, Italy

[3] Consorzio INSTM, Via Giusti 9, 50121 Florence, Italy; E-Mail: stefano.caporali@unifi.it

† This paper is an extended version of our paper published in the 42nd Lunar and Planetary Science Conference, The Woodlands, TX, USA, 7–11 March 2011.

‡ These authors contributed equally to this work.

* Author to whom correspondence should be addressed; E-Mail: vanni.moggicecchi@unifi.it; Tel.: +39-055-275-7456; Fax: +39-055-275-6322.

Academic Editor: Jesus Martinez-Frias

Received: 1 April 2015 / Accepted: 23 June 2015 / Published: 2 July 2015

Abstract: A comprehensive classification of primitive achondrites is difficult due to the high compositional and textural variability and the low number of samples available. Besides oxygen isotopic analysis, other minerochemical and textural parameters may provide a useful tool to solve taxonomic and genetic problems related to these achondrites. The results of a detailed modal, textural and minerochemical analysis of a set of primitive achondrites are presented and compared with literature data. All the samples show an extremely variable modal composition among both silicate and opaque phases. A general trend of troilite depletion *vs.* silicate fraction enrichment has been observed, with differences among coarse-grained and fine-grained meteorites. In regard to the mineral chemistry, olivine shows marked differences between the acapulcoite-lodranite and winonaite groups, while a compositional equilibrium between matrix and chondrules for both groups, probably due to the scarce influence of metamorphic grade on this phase, was

observed. The analysis of Cr and Mn in clinopyroxene revealed two separate clusters for the acapulcoite/lodranite and winonaite groups, while the analysis of the reduction state highlighted three separate clusters. An estimate of equilibrium temperatures for the acapulcoite-lodranite and winonaite groups is provided. Finally, proposals regarding the genetic processes of these groups are discussed.

Keywords: primitive achondrites; acapulcoite; lodranites; winonaites; X-ray maps

1. Introduction

Primitive achondrites are considered transitional products between chondrites and differentiated meteorites and are thought to derive from chondritic ancestors that suffered a medium-grade thermal metamorphism and partial fusion [1].

According to the most recent theories these meteorites originated inside small asteroids that underwent accretion and differentiation processes before being destroyed by catastrophic collisions that lead to a more or less rapid cooling of the nascent material [1,2]. This theory would justify the presence of structures displaying different partial fusion, metamorphism and recrystallization rates, like relict chondrules found in some of these samples. A comprehensive and exhaustive classification of primitive achondrites has never been performed due to the high compositional and textural inhomogeneity and the low number of samples available. Acapulcoites display a fine-grained texture (mean grain size 150–300 μm) consisting of olivine and pyroxene, with minor plagioclase, sulfides and Fe/Ni alloys [3]. The presence of metal or sulfide veins and of relict chondrules, as well as the chondritic amount of plagioclase and the depletion in troilite and metal suggests a low fusion grade (1%–5%) at temperatures of about 950–1000 °C, as also indicated by trace element analysis [4,5]. The fine texture of mafic silicates can be explained through solid state diffusion and crystallization processes [3]. Lodranites, although chemically similar to acapulcoites, display markedly different textural features, being much coarser grained (mean grain size 300–700 μm) and containing a lower amount of plagioclase and sulfides. It has been suggested that they suffered a much higher metamorphic grade (10%–15% according to [6]); 25% according to [5]), corresponding to temperatures of about 1050–1200 °C [3], that allowed a higher recrystallization rate and, consequently, a coarser grain size than the acapulcoites. The absence of chondrules is consistent with such a hypothesis [7]. Their mineralogical composition is depleted in those phases, like plagioclase, sulfides and Fe/Ni alloys, which may have been transformed into liquid and removed from the system. This hypothesis is confirmed by the trace element composition which displays a marked depletion in lithophile incompatible elements, especially rare earth elements (REE) [5,8].

Although it is well-established that lodranites experienced higher temperatures than acapulcoites, the origin of such temperatures is not clear. The radioactive decay of short-lived isotopes like ^{27}Al, typical of the first stages of formation of the Solar System, cannot be considered the only heat source due to its slow heating and subsequent cooling rates which should produce a much more homogeneous rock, both texturally and compositionally, as compared to acapulcoites and lodranites. A process resulting from impacts has therefore invoked to explain the local heating of the parental body and the

mixing of evolved and primitive portions [1,2]. Traces of such collisions may be the presence of troilite veins and of shock features in olivine crystals [1,7,9]. These features are more common in acapulcoites than in lodranites, which experienced a higher metamorphic grade. Recently, several reports have focused on the ^{182}Hf–^{182}W chronometry to reveal the early evolution history in the acapulcoite-lodranite parent body [10,11], while others have focused on the I–Xe system to determine the accretion age of the acapulcoite-lodranite parent body, suggesting the existence of post-formation collision events [12]. The affinity of lodranites for acapulcoites appears evident from the isotopic distribution of oxygen, supporting the hypothesis that they originated from a common parent body. According to this hypothesis acapulcoites are representative of the outer, less thermally metamorphosed, portion of the parent body and lodranites are representative of the inner, highly metamorphosed zones. This hypothesis is in agreement with geochemical data [4]. Acapulcoites and lodranites are therefore considered end-members of the same series, although intermediate products, like LEW 86220 [13–15] and Y-74357 [16], are extremely rare.

An evolution scheme has been proposed [17], which considers, in a progressive heating process, the following steps: primitive acapulcoites, typical acapulcoites, transitional acapulcoites, enriched acapulcoites and lodranites. Each step is characterized by a partial loss of sulfides (first step) or silicates (following steps). An attempt to solve this classification complexity has been made by comparing LREE values [17]. Better results have been obtained using the Zr and Ti contents of ortho- and clinopyroxenes [8], even if this cannot be considered a secure classification parameter due to the high analytical uncertainty. Other parameters, like Se partitioning [18,19], or the LREE in ortho- and clinopyroxenes did not provide reliable results.

The other group of primitive achondrites contains winonaites and the silicate inclusions in the iron meteorites of the IAB group, which are considered to represent different regions of the same parental body [20]. Even in this case the group contains both more primitive and more evolved members, displaying evidence of a fusion and differentiation process on the parental body. The presence of moderate fractionation of both siderophile and lithophile elements suggests a chondritic affinity, although the contents of the lithophile elements are more variable respect to those observed in the acapulcoite-lodranite clan [20]. The studies on the age of formation suggest that these meteorites are coeval to acapulcoites-lodranites and that their initial formation stage is similar, with regions of the parent body that reached high metamorphic grade temperatures and a subsequent diffuse recrystallization, whereas other regions proceeded further, achieving partial fusion temperatures [20–23]. Nevertheless, the final formation stage appears quite different, with regions in which the molten metal mixed to silicates and formed the silicate-inclusion-rich IAB iron meteorites and other regions, which formed winonaites, that were not subject to this process [24]. Based on W and Sm isotope measurements for metals and silicates of non-magmatic iron meteorite groups and winonaites, their exposure history and parent body formation has been assessed [25]. A metal separation at 5.06 $^{+0.42}/_{-0.41}$ Ma after the solar system formation was proposed, which agrees with the previously published ^{182}Hf–^{182}W ages for both the silicate melting (4.6 $^{+0.7}/_{-0.6}$ Ma) and the formation of winonaites (4.8 $^{+3.1}/_{-2.6}$ Ma) and corresponds to an accretion age of ~2 Ma after Solar System formation for the IAB/winonaite parent body [10]. The metamorphism of IAB silicate inclusions and winonaites has been reported to take place at significantly different times, between ~11 and ~14 Ma, via an impact triggered melt pool formation process [25]. Currently, the main parameter used for the classification of primitive achondrites is the

isotopic composition of oxygen. As revealed by the oxygen isotope (OI) data, samples belonging to the two groups (acapulcoites-lodranites and winonaites-IAB silicate inclusions) are located in two distinct areas below the terrestrial fractionation line, suggesting an origin from separate parent bodies [26,27]. It is important to stress that this method may be, in some cases, partially affected by terrestrial contamination, especially where desert samples are concerned. It is, therefore, crucial to complement OI data with other geochemical and textural parameters. Herein we suggest the use of a new tool based on minerochemical and textural parameters that may be useful to solve taxonomic and genetic problems related to primitive achondrites [1,2]. In order to determine these parameters a detailed modal, textural and minerochemical analysis regarding both the matrix and the chondrules of a set of 18 meteorites belonging to primitive achondrites has been performed and the results have been compared with literature data [4,13,14,17,28] on these and other primitive achondrites.

2. Materials and Methods

Optical microscopy and imaging have been performed at the laboratories of the Museo di Scienze Planetarie di Prato by means of a Axioplan-2 polarizing optical microscope equipped with Axiocam-HR camera and Axiovision 4.1 software. SEM-EDX X-ray maps have been performed at the Dipartimento di Chimica dell'Università di Firenze by means of a Hitachi SEM model S-2300 operating at 25 kV, 15 nA, 1 μm of spot diameter and equipped with a Si(Li) EDX analyzer and a Noran System Six 300 software. EMPA-WDS analyses have been performed at the Padova laboratories of the IGG–CNR (National Council of Research) with a Cameca Camebax Microbeam microprobe operating at 20 kV, 20 nA and 1 μm of spot diameter.

X-ray maps have been performed at a high definition (1024 × 812 pixels) with total acquisition time of 25 min for each map. The modal analyses have been extracted from elemental X-ray maps using the image analysis tool of the Noran System Six 300 software which provides the areal distribution of the selected element by means of the processing of its pixels # *vs.* net counts histogram. Repeated measures on the same area provided a maximum error of 10%. Measurements have been performed on at least three 3 × 2 mm^2 areas per sample, averaging the results. The mineralogical phases have been then quantified on the basis of the surface percentage amount of selected elements, according to the correspondence scheme presented in Table 1: for example olivine and pyroxene have been quantified based on the amount of Mg, while the Fe/Ni alloys and Fe-oxides have been discerned on the basis of the gray scale in the back-scattered electrons (BSE) image mode.

The list of the thin sections analyzed and of the institutions that provided the samples is reported, together with their classification, in Table 2.

Figure 1 reports an example of a multi-elemental X-ray map performed on a chondrule of the sample Y-74025.

Table 1. Correspondence scheme between the quantified mineralogical phases and the elements detected.

Element	Mineral Phases
Si	Silicates
S	Sulfides
Fe	Fe/Ni alloys and secondary oxides
Al	Plagioclase
Ca	Apatite and clinopyroxene
P	Apatite
Mg	Olivine and orthopyroxene

Table 2. List of the thin sections studied and of the institutions that provided the samples; MSP = Museo di Scienze Planetarie della Provincia di Prato; NHM = Natural History Museum of London; Hamb = Mineralogisches Museum, Universität Hamburg; JSC-ARES = Johnson Space Center—Astromaterial Research and Exploration Science; AMRC-NIPR = Antarctic Meteorite Research Center—National Institute for Polar Research; Vernad = Vernadsky Institute of Geochemistry and Analytical Chemistry; UCLA = University of California, Los Angeles.

Meteorite Name	Thin Section Label	Classification	Institution
Allan Hills 81187	ALH 81187	acapulcoite	JSC-ARES
Allan Hills 81261	ALH 81261	acapulcoite	JSC-ARES
Allan Hills 77081	ALHA77081-11-8	acapulcoite	JSC-ARES
Asuka 881902	A881902-141-3	acapulcoite	AMRC-NIPR
Dhofar 290	DHO 290	acapulcoite	Vernad
Graves Nunataks 98028	GRA 98028	acapulcoite	JSC
Northwest Africa 1052	MSP 2377	acapulcoite	MSP
Northwest Africa 1054	MSP 2378	acapulcoite	MSP
Northwest Africa 3008	NWA 3008	acapulcoite	Hamb
Northwest Africa 1058	MSP 2264	winonaite	MSP
Northwest Africa 1463	UCLA NWA 1463	winonaite	UCLA
Pontlyfni	BM1975, M6 P6851	winonaite	NHM
Queen Alexandra Range 94535	QUE 94535	winonaite	JSC-ARES
Yamato 74025	Y74025-52-1	winonaite	AMRC-NIPR
Yamato 74063	Y74063-52-4	acapulcoite	AMRC-NIPR
Yamato 74357	Y74357-62-1	lodranite	AMRC-NIPR
Yamato 791491	Y791491-51-1	lodranite	AMRC-NIPR
Yamato 8005	Y8005-51-3	winonaite	AMRC-NIPR

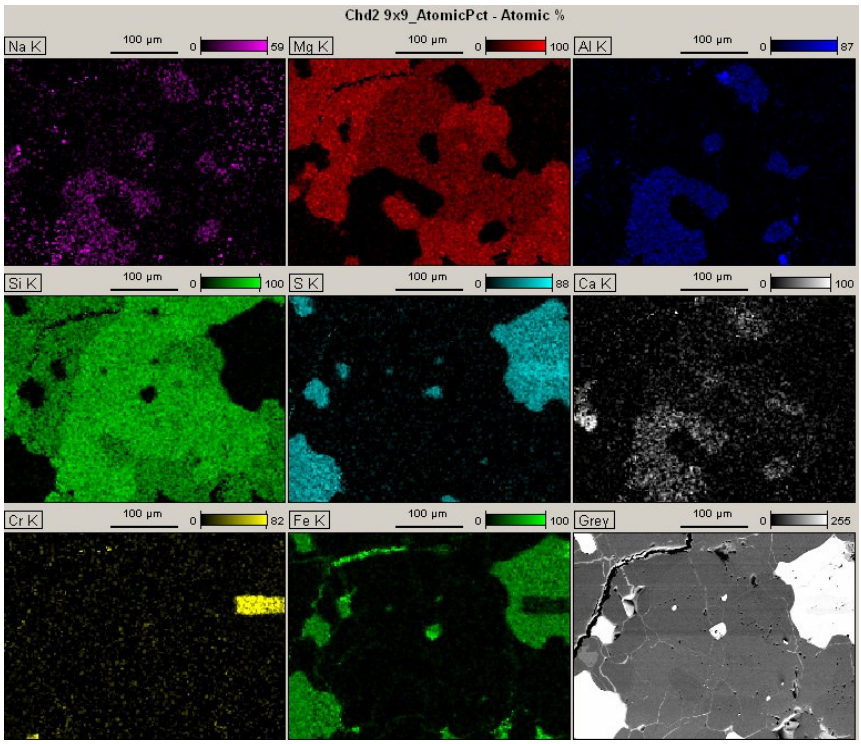

Figure 1. BSE scanning electron photomicrograph (bottom right) and X-ray compositional maps of the elements Na, Mg, Al, Si, S, Ca, Cr and Fe in a chondrule of the sample Y-74025 (winonaite). The color intensity is proportional to the amount of the element present. Mineral phases can be identified following the scheme reported in Table 1.

3. Results and Discussion

3.1. Textural Features

Primitive achondrites display an extremely wide textural variability due to the fact that some of them contain chondrules set in a fine grained matrix, while others have no chondrules and show a fine- or a coarse-grained texture. Representative examples of the typical textures are shown in Figure 2. Meteorites indicated with the letters from (A) to (I) display a fine-grained texture and relict chondrules; those from (L) to (Q) have a variable grain size from fine to medium; those from (R) to (T) are characterized by a markedly coarse grain size.

The modal analysis is conventionally performed by means of optical microscope images. This method is not particularly suitable for primitive achondrites as they are often characterized by a fine grained texture, which impedes an accurate determination of grain size. Therefore, the modal analysis of the mineral phases used herein has been obtained by means of image analysis of the X-ray maps performed on the investigated meteorites. X-ray maps can provide a very high spatial resolution (below 5 µm) that allows detection also of very small grains (mean size < 50 µm), that can be therefore included in the count. This method has also been applied to the microcrystalline structures typical of the chondrules, allowing a comparison between the modal composition of the chondrules and of the surrounding matrix. The results presented in Table 3 regard the matrix and display the mean values obtained from modal analyses performed on 3–5 different areas of 3 × 2 mm^2 for each sample. The selected areas are representative of the typical texture of the matrix.

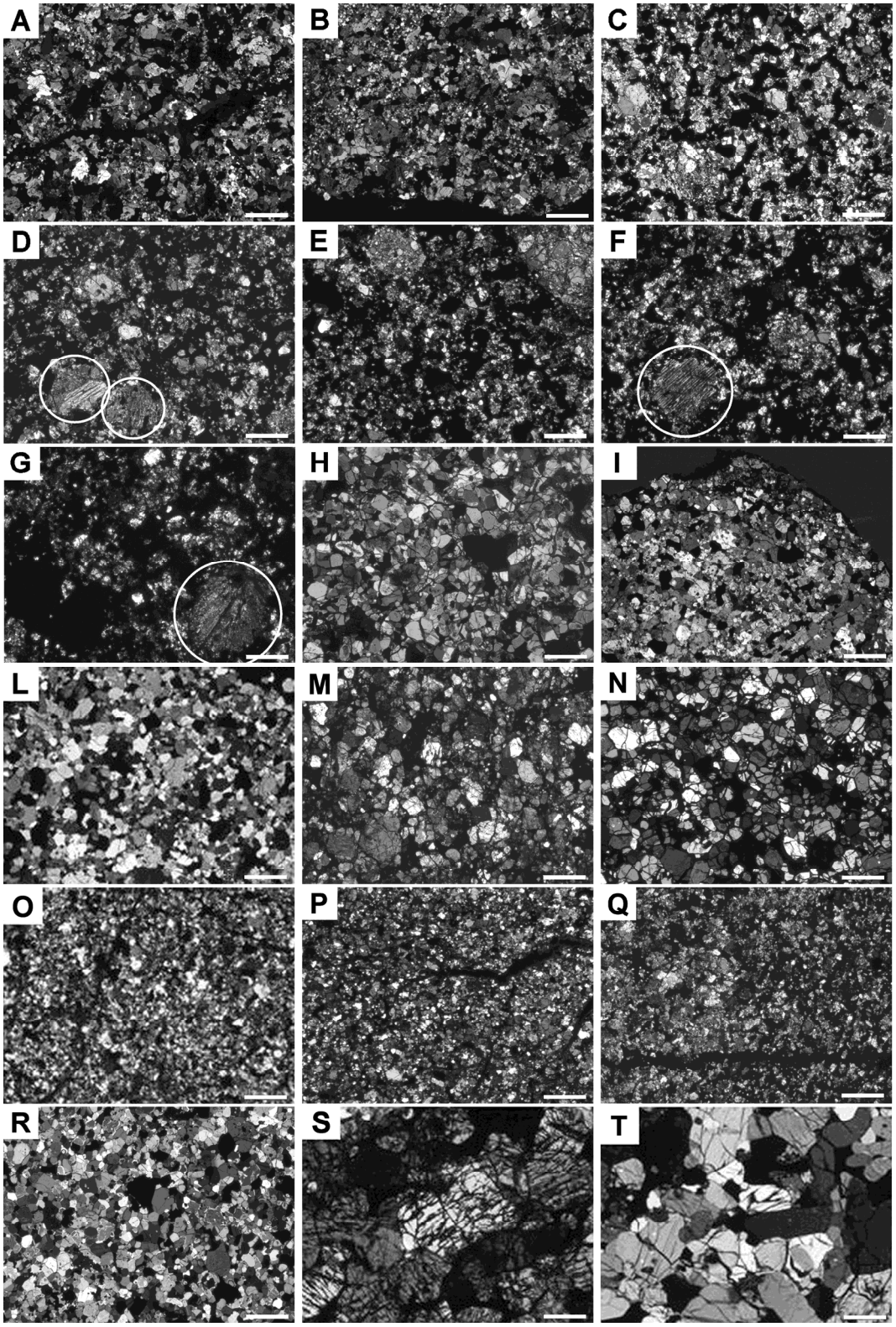

Figure 2. Photomicrographs of the thin sections of the meteorites investigated in the present study: (**A**) A-881902; (**B**) Y-74063; (**C**) GRA 98028; (**D**) NWA 1052; (**E**) NWA 1054; (**F**) NWA 1058; (**G**) NWA 1463; (**H**) NWA 3008; (**I**) Y-74025; (**L**) ALHA77081; (**M**) ALH 81187; (**N**) DHO 290; (**O**) QUE 94535; (**P**) Y-8005; (**Q**) Pontlyfni; (**R**) ALH 81261; (**S**) Y-74357; (**T**) Y-791491; transmitted light, crossed polars; scale bar is 500 μm. Chondrules are highlighted with white circles.

Table 3. Modal distribution of mineralogical phases as determined by analysis of X-ray map images; all values are in %; error is 2σ; sample classification is reported in Table 2.

Mineral Phases	Samples																	
	Yamato 74357	**Yamato 791491**	**Yamato 8005**	**QUE 94535**	**ALH 81187**	**ALH 81261**	**ALHA 77081**	**Yamato 74025**	**Yamato 74063**	**GRA 98028**	**Asuka 881902**	**NWA 1052**	**NWA 1054**	**NWA 3008**	**NWA 1058**	**NWA 1463**	**DHO 290**	**Pontlyfni**
Silicates	83.0 ± 7	77.3 ± 10	54.7 ± 10	84.3 ± 4	82.4 ± 4	87.5 ± 6	83.7 ± 2.3	86.9 ± 3	86.2 ± 5	69.8 ± 3	79.1 ± 6	84.2 ± 5	85.6 ± 5	89.5 ± 5	63.6 ± 5	49.3 ± 6	79.8 ± 5	67.1 ± 5
Opaque phases	17.7 ± 10	21.3 ± 10	44.5 ± 8	15.3 ± 1	16.8 ± 3	12.1 ± 5	14.4 ± 2.3	11.6 ± 3	16.0 ± 2	30.3 ± 3	22.0 ± 8	15.8 ± 2	16.1 ± 2	10.5 ± 1	27.1 ± 2	51.1 ± 10	24.5 ± 3	33.8 ± 2
Fe/Ni alloys	13.4 ± 10	14.1 ± 8	12.2 ± 10	1.4 ± 1	6.0 ± 3	5.5 ± 4	8.8 ± 2.1	2.5 ± 1	4.6 ± 2	3.9 ± 3	3.3 ± 1	4.2 ± 2	3.2 ± 2	2.1 ± 1	13.1 ± 3	42.9 ± 8	7.1 ± 2	10.9 ± 2
Troilite	0.4 ± 0.1	2.4 ± 0.4	5.8 ± 0.5	6.5 ± 2	1.9 ± 1	5.9 ± 3	5.6 ± 0.6	8.2 ± 3	8.4 ± 1.4	16.3 ± 2	14.5 ± 2	6.2 ± 1.5	7.5 ± 2	3.2 ± 1	7.0 ± 2	4.0 ± 2	5.6 ± 2	19.1 ± 2
Oxides	3.9 ± 0.7	4.8 ± 1	26.5 ± 4	7.3 ± 3	9.0 ± 2	0.8 ± 0.3	n.d.	0.7 ± 0.2	3.0 ± 2	10.2 ± 2	4.2 ± 2	5.3 ± 2	5.3 ± 1.5	5.3 ± 2	7.0 ± 2	4.3 ± 2	11.6 ± 2	3.9 ± 1.5
Diopside	2.5 ± 1.2	0.5 ± 0.1	5.1 ± 2	3.1 ± 1	0.8 ± 0.2	7.0 ± 1	3.2 ± 1.1	7.3 ± 0.3	5.9 ± 1.4	6.5 ± 2	4.6 ± 2	5.3 ± 1.5	5.3 ± 1.3	10.5 ± 2	6.4 ± 1	4.3 ± 2	2.0 ± 2	5.0 ± 1.5
Plagioclase	n.d.	n.d.	7.7 ± 3	7.8 ± 0.6	6.6 ± 1.5	13.2 ± 3	12.8 ± 1.4	14.5 ± 1.4	13.1 ± 3	10.4 ± 2	12.6 ± 3	15.8 ± 3	16.0 ± 2	15.8 ± 2	9.6 ± 2	4.3 ± 3	9.3 ± 3	9.1 ± 3
Olivine	65.3 ± 5	31.3 ± 7	11.6 ± 5	24.5 ± 5	32.7 ± 7	25.5 ± 2	26.7 ± 2.2	21.2 ± 3	24.0 ± 3.5	26.6 ± 6	24.9 ± 3	26.3 ± 4	26.7 ± 3	36.8 ± 4	33.8 ± 4	18.8 ± 2	30.3 ± 5	32.0 ± 4
Orthopyroxene	15.2 ± 7	43.6 ± 1	29.6 ± 3	48.2 ± 5	39.6 ± 10	40.2 ± 1	38.8 ± 1.0	43.0 ± 3	41.1 ± 2	27.5 ± 4	37.6 ± 5	36.8 ± 3	37.4 ± 3	26.3 ± 2	18.8 ± 2	21.4 ± 5	36.8 ± 3	21.0 ± 3
Chromite	n.d.	1.5 ± 1	0.3 ± 0.1	n.d.	0.1 ± 0.2	1.1 ± 0.8	1.9 ± 1.6	0.1 ± 0.1	0.3 ± 0.1	0.4 ± 0.2	0.1 ± 0.1	0.1 ± 0.1	0.5 ± 0.1	n.d.	0.4 ± 0.1	n.d.	n.d.	n.d.
Apatite	n.d.	n.d.	n.d.	n.d.	0.4 ± 0.2	0.4 ± 0.1	0.4 ± 0.1	n.d.	0.7 ± 0.1	1.2 ± 1	0.3 ± 0.1	n.d.	0.4 ± 0.1	n.d.	1.2 ± 0.8	1.4 ± 0.3	0.3 ± 0.1	n.d.
Weathering *	22.3 ± 10	20.2 ± 10	39.6 ± 7	32.1 ± 9	35.5 ± 10	7.3 ± 3.0	n.d.	5.6 ± 2	16.1 ± 7	26.1 ± 6	17.0 ± 4	26.3 ± 4	26.7 ± 5	35.1 ± 6	22.1 ± 6	8.3 ± 3	33.8 ± 5	10.1 ± 4

Note: * weathering is calculated as % of the secondary oxides with respect to the total amount of opaque phases.

All the samples display an extremely variable modal composition and no clear groups can be singled out: silicates account for 50% to 80% of the total volume, with olivine and orthopyroxene as major phases. Opaque phases are considered as the sum of troilite, Fe/Ni alloys and oxides. It is important to stress that the large error values reported in Table 3 are mainly due to the high inhomogeneity of the samples rather than to the analytical method. The high variability in the modal composition shown by these samples, that has been noted previously [22,29,30], does not affect the petrographic valence of the analysis since it reflects the complex magmatic processes that these meteorites have undergone.

A plot of the troilite/silicate ratio (in vol %) *versus* the total silicate vol % enables a number of interesting observations to be made. Besides the general trend of relative depletion of the total amount of troilite related to the enrichment of the silicate fraction, a peculiar feature can be observed if the overall texture is considered (Figure 3): coarse grained meteorites displaying an equigranular texture with marked 120° triple junctions, thus indicating a high metamorphic degree, are located in the bottom right portion of the plot (empty circles), while fine-grained meteorites, regardless of whether they contain relict chondrules, are located in the upper left portion of the diagram (full circles).

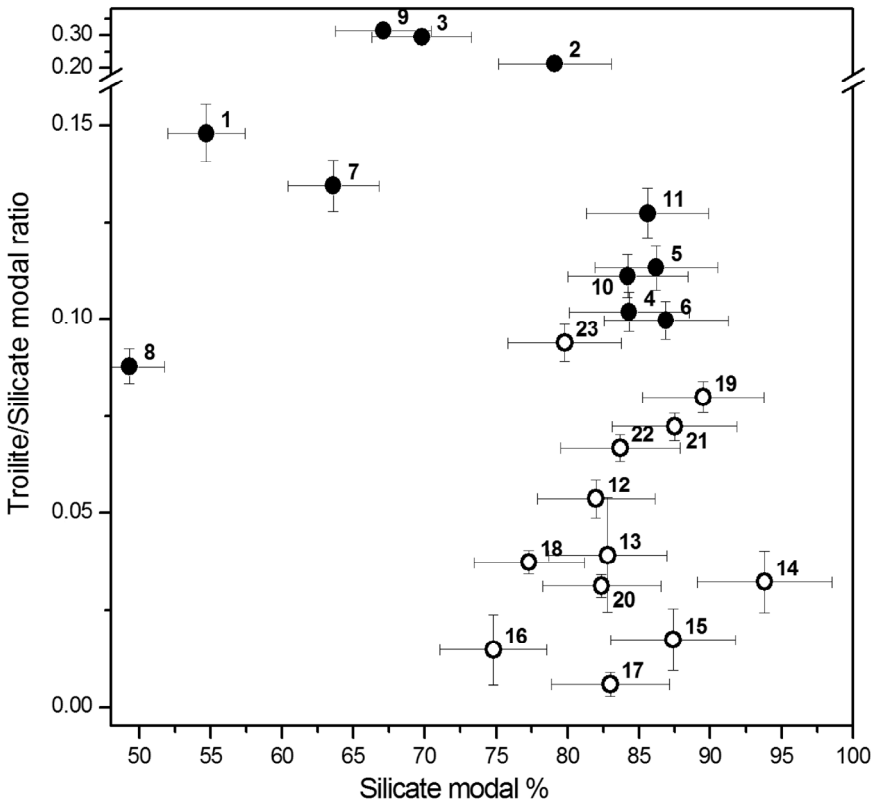

Figure 3. Diagram displaying the troilite/silicate ratio as a function of the total modal amount of silicates. Numbers refer to samples as indicated: 1 = Y-8005; 2 = ALH 881902; 3 = GRA 98028; 4 = QUE 94535; 5 =Y-74063; 6 = Y-74025; 7 = NWA 1058; 8 = NWA 1463; 9 = Pontlyfni; 10 = NWA 1052; 11 = NWA 1054; 12 = TIL 99002; 13 = Superior Valley; 14 = MAC 88177; 15 = LEW 88280; 16 = EET 84302; 17 = Y-74357; 18 = Y-791491; 19 = NWA 3008; 20 = ALH 81187; 21 = ALH 81261; 22 = ALHA77081; 23 = DHO 290. Fine and coarse grained meteorites are depicted by full and empty circles, respectively. See Table 2 for sample classification. Data for samples 12–16 are from previous reports [1,17].

Another interesting trend can be highlighted by plotting the sialic/mafic silicates ratio *versus* the total amount of silicates. The meaning of this plot is based on the ground that since in the partial fusion of a chondritic parental body the first silicate liquid phase produced is mainly constituted by sialic components (plagioclase), the residual solid results enriched in mafic components (olivine and pyroxene [5]). In our case, the data reported in Figure 4 show that lodranites are strongly depleted in sialic silicates and appear well separated from the other primitive achondrites, whereas no meaningful trends are clearly detected for acapulcoites and winonaites.

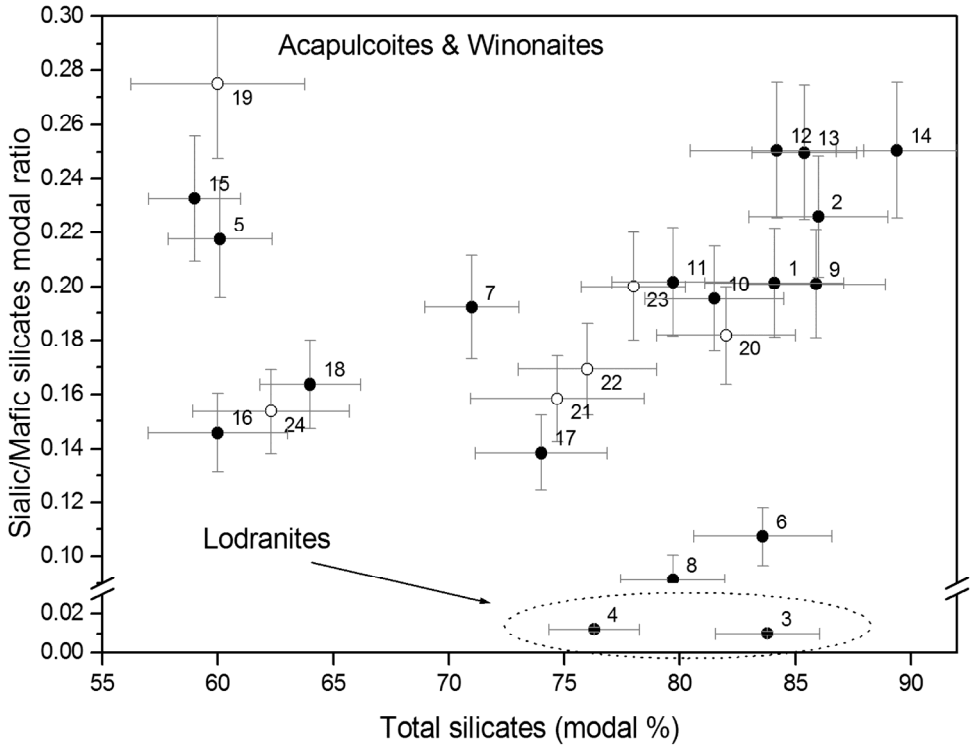

Figure 4. Plagioclase/mafic silicate ratio as a function of the total amount of silicates; full circles are data of this study, empty circles literature data (samples from 19 to 24). Numbers refer to samples as indicated: 1 = Y-74063; 2 = Y-74025; 3 = Y-74357; 4 = Y-791491; 5 = Y-8005; 6 = QUE 94535; 7 = GRA 98028; 8 = ALH 81187; 9 = ALH 81261; 10 = ALHA77081; 11 = A-881902; 12 = NWA 1052; 13 = NWA 1054; 14 = NWA 3008; 15 = NWA 1058; 16 = NWA 1463; 17 = DHO 290; 18 = Pontlyfni; 19 = NWA 725; 20 = TIL 99002; 21 = Monument Draw; 22 = Mt. Morris; 23 = Y-75300; 24 = Y-75305. See Table 2 for sample classification.

Moreover, a separate modal analysis comparing the chondrules and adjacent areas of the matrix has been performed on 6 of the investigated meteorites, in order to shed light on some petrogenetic features of these meteorites. The results obtained on each meteorite are presented in Table 4 and discussed below.

GRA 98028:

In this meteorite the intrachondrule texture is extremely fine-grained, and the chondrules contain several minute metal-sulfide aggregates and are often rimmed by metal/sulfide ponds. They range in

size from 200 to 800 μm. The modal analysis shows that the chondrules are silicates, especially orthopyroxene, enriched and depleted in opaques compared with the matrix.

Y-74063:

In this meteorite, the chondrules are relatively uncommon and smaller (200 to 500 μm) than in GRA 98028. The few chondrules observed display a markedly coarse-grained texture. The modal analysis highlighted an enrichment in ortho- and clinopyroxenes, and a depletion in opaque phases compared with the matrix. Nevertheless, the olivine and the plagioclase contents are similar. These results suggest that the meteorite underwent a higher metamorphic degree if compared to GRA 98028, as confirmed by the coarser texture.

Y-74025:

This meteorite displays smaller (300–500 μm) and coarser-grained chondrules. The modal composition of chondrules appears to be enriched in olivine and depleted in orthopyroxene, while no differences of the opaque phases with respect to the matrix can be observed.

A-881902:

This sample displays a high number of chondrules with extremely variable sizes (300–800 μm), shapes and types: some chondrules have a typical chondritic, fine-grained radial texture, while others show large crystals with 120° triple junctions, typical of higher metamorphic degrees. This variability is not confirmed by the modal analysis data since neither marked enrichments nor depletions are visible among silicate and opaque phases indicating on the whole higher metamorphic degree conditions.

NWA 1058:

As previously reported [31], this meteorite is characterized by a high number of relict chondrules, with large sizes (800–1500 μm), rounded shapes and fine-grained textures. The modal analysis performed on these chondrules highlighted an enrichment in silicates (namely orthopyroxene and olivine) and a depletion in opaque phases, mainly distributed as tiny aggregates of sulfides and Fe/Ni alloys in peripheral areas of porphyritic pyroxene (PP) chondrules or as large blebs at chondrules boundaries in porphyritic olivine-pyroxene (POP) chondrules.

NWA 1463:

The chondrules of this meteorite display sub-rounded shapes and radial, very fine-grained textures. Two different types of chondrules have been detected, hereafter named C1 and C2. The C1-type have unequigranular textures with large olivine crystals surrounded by a fine-grained matrix consisting of ortho- and clino-pyroxenes. The C2-type display an equigranular texture, with diopside homogeneously distributed. This textural feature has been confirmed by the compositional maps: the distribution of Ca reflects the textural observation, with C1-type chondrules displaying an enrichment in orthopyroxene and plagioclase if compared with the clinopyroxene-rich matrix, and C2-type chondrules showing an

enrichment in clinopyroxene and plagioclase compared with the orthopyroxene-rich matrix. Similarly to the previous cases, all the chondrules are depleted in opaque phases.

Table 4. Modal analysis of chondrule-bearing samples; chondrule data ranges are compared with the corresponding matrix mean values (in brackets). Opaques are considered as the sum of Fe/Ni alloys, troilite and oxides. See Table 2 for meteorite classification.

Meteorite Name	N° of Chondrules	Chondrules Dimensions' ranges (μm)	Modal Abundances (%)								
			Silicates	Opaques	Fe/Ni Alloys	Troilite	Oxides	Diopside	Plagioclase	Olivine	Orthopyroxene
GRA 98028	5	200–800	74–87 (70)	8–28 (30)	2–4 (4)	5–14 (16)	3–15 (10)	4–9 (7)	10–15 (10)	21–33 (27)	25–46 (28)
Y-74063	3	200–500	93–95 (86)	3–8 (16)	0–1 (5)	2–6 (8)	1–6 (3)	9–22 (6)	9–14 (13)	13–26 (24)	44–54 (41)
Y-74025	4	300–500	80–85 (87)	13–19 (12)	0–4 (3)	9–18 (8)	0–1 (1)	1–12 (7)	10–17 (15)	30–41 (21)	17–32 (43)
A-881902	5	300–800	76–85 (79)	8–13 (22)	0–4 (3)	2–12 (15)	2–3 (4)	2–9 (5)	7–14 (13)	25–34 (25)	28–36 (38)
NWA 1058	2	800–1500	82–90 (64)	8–16 (27)	6–12 (13)	2–4 (7)	0–12 (7)	2–10 (6)	1–12 (10)	37–38 (34)	20–50 (19)
NWA 1463	2	1250–1500	30–55 (49)	4–14 (51)	2–12 (43)	2 (4)	2 (4)	8–85 (4)	15–23 (19)	4–8 (21)	10–25 (17)

3.2. Mineral Chemistry

In order to determine taxonomically meaningful minerochemical parameters, a detailed EMPA study has been performed of both major and minor elements of selected mineral phases (plagioclase, diopside, orthopyroxene and olivine).

3.2.1. Plagioclase

Analyses have been performed both on crystals of the chondrules-free areas and on those inside chondrules. In regard to the matrix, a mean of 7–10 plagioclase crystals for each meteorite have been analyzed. Plagioclase displays an albitic composition ($An_{13–24}Or_{1–6}$), with no significant variability inside each sample. Even the differences among the samples does not suggest any relationship with the meteorite class, therefore being of no benefit for taxonomic purposes. The data from the analyses performed on chondrules also suggests the absence of any trend, except for those from the meteorite NWA 1463 in which plagioclase in chondrules is much more Ca-rich ($An_{29±2}$ and $Or_{5±1}$) than that in the matrix ($An_{13±1}$ and $Or_{5±1}$). That is probably attributable to the lower metamorphic degree suffered by this meteorite.

3.2.2. Olivine

Quantitative EMPA analyses have been performed on olivine crystals in both matrix and chondrule areas. The molar contents of Fa, Fo and Tf calculated revealed a marked difference between winonaites, which display a forsteritic composition (Fo ≥ 98), and acapulcoite-lodranites, which were

Mg-depleted (Fo = 84–96), in good agreement with literature data [17,32,33]. Nevertheless, this compositional feature cannot be unequivocally related to the two different groups and has to be considered a first, not crucial, indication. The analyses performed on chondrule crystals showed no marked differences compared with matrix data, with a compositional variability lower than that existing among the different meteorites. These results are unsurprising for equilibrated products like lodranites, but are quite interesting if referred to acapulcoites and winonaites, which underwent a lower metamorphic degree.

Other minor elements, like Mn and Cr, display trends typically related to the petrologic evolution of the meteorite. In particular, as has been previously suggested [34], the decreasing MnO/FeO ratio is related to reduction processes suffered by the meteorite. Some acapulcoites display high values ($Fa_{25–32}$ mol %), similar to those of chondrites, while others show much lower values ($Fa_{18–20}$ mol %), achieving extremely low values for winonaites ($Fa_{1–3}$ mol %) [1,35].

The Fe/Fe+Mg (Fe#) data obtained on the studied meteorites are in good agreement with literature data: as highlighted in Figure 5, all the data display a positive linear correlation (R = 0.979). The most reduced samples, like winonaites, are located in the lower-left portion of the graph, allowing a clear identification of this group.

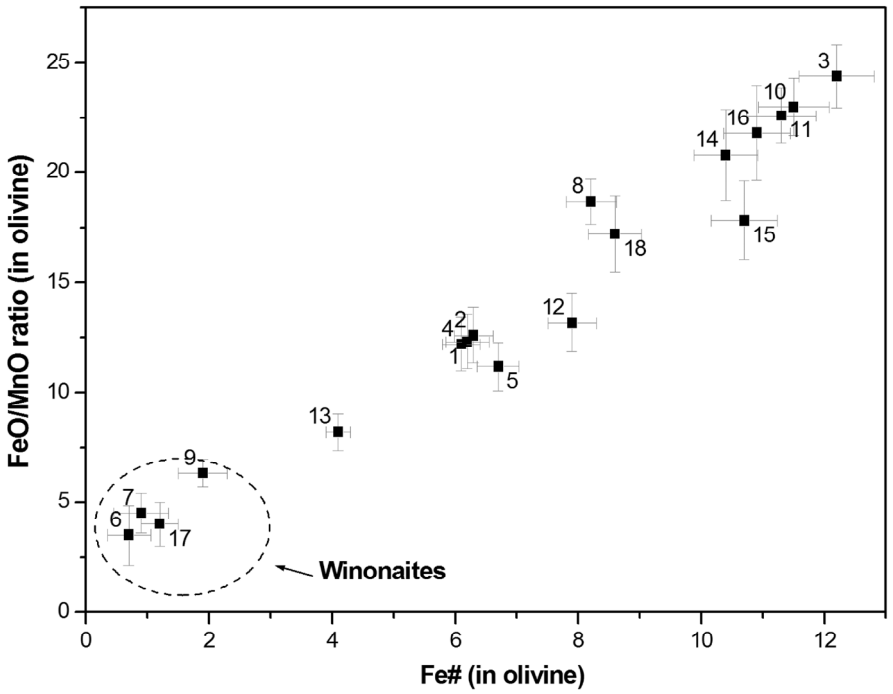

Figure 5. Plot of the FeO/MnO ratio *versus* the Fe# content in olivine. Numbers refer to samples as indicated: 1 = NWA 1052; 2 = NWA 1054; 3 = NWA 3008; 4 = NWA 1463; 5 = NWA 1058; 6 = Pontlyfni; 7 = QUE 94535; 8 = GRA 98028; 9 =Y-74025; 10 = Y-791491; 11 = Y-74063; 12 = Y-74357; 13 = ALH 81187; 14 = ALH 81261; 15 = ALHA77081; 16 = Dho 290; 17 = Y-8005; 18 = A-881902; see Table 2 for sample classification.

3.2.3. Pyroxene

The EMPA analyses of the major elements performed on pyroxenes allowed the overall composition of the samples to be defined: in a classic 4-sided pyroxene diagram (En-Fs-Hed-Dio) all

the samples are positioned near the diopside corner and display a narrow compositional range with slight differences among groups that confirm the linear distribution observed for olivine: winonaites show an Mg-rich composition (mean value $Fs_{50}En_6Wo_{44}$), lodranites a Fe-rich one (mean $Fs_{52}En_1Wo_{47}$), while acapulcoites display intermediate values.

The analysis of the minor elements provided the most interesting results: a plot of the Cr content of diopside *versus* Mg/Fe+Mg (Mg#) of olivine (Figure 6) shows that winonaites are characterized by lower values of Cr (<1% of Cr_2O_3) and higher values of Mg# (>98). Two separate clusters of values corresponding to the acapulcoite/lodranite and winonaite groups can be therefore identified, in agreement with literature data [22,30,36]. Analogous results have been obtained plotting the Mn content *versus* the Mg# of olivine, although an overlapping area can be observed in the central portion of the data distribution, suggesting that the Mn content is a less distinguishing feature than Cr. From a minerogenetic point of view, the lower content of Cr in diopside is consistent with the more reduced environment in which winonaites formed, due to the higher reduction potential of this element in comparison with Fe. It is important to stress that the less reduced state of the acapulcoite-lodranite group is somewhat surprising considering that these meteorites were subjected to a higher metamorphic degree. This is confirmed by the previously described textural features, like the coarser grain size and the presence of 120° triple junctions, as well as by the partial loss of the sulfides and of the sialic-silicate fraction. An alternative process of shock-induced selective O depletion can be therefore hypothesized.

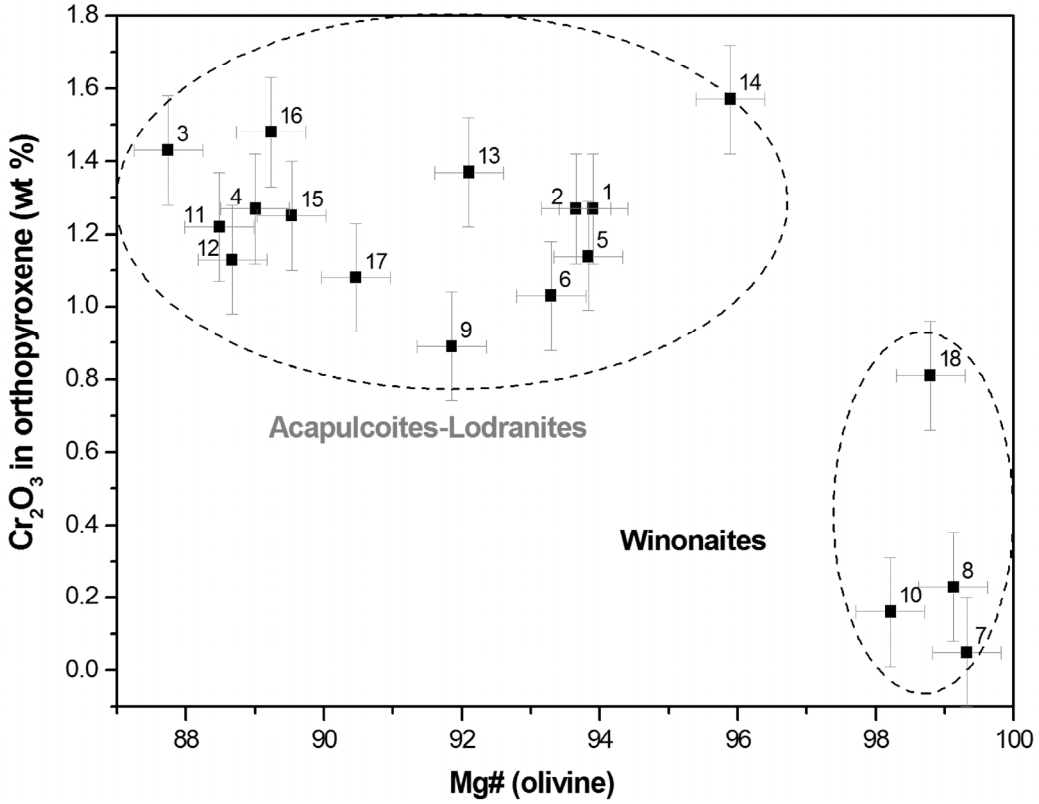

Figure 6. Plot of the Cr_2O_3 content in orthopyroxene *versus* the Mg# in olivine. Numbers refer to samples as indicated: 1 = NWA 1052; 2 = NWA 1054; 3 = NWA 3008; 4 = Dho 290; 5 = NWA 1463; 6 = NWA 1058; 7 = Pontlyfni; 8 = QUE 94535; 9 = GRA 98028; 10 = Y-74025; 11 = Y-791491; 12 = Y-74063; 13 = Y-74357; 14 = ALH 81187; 15 = ALH 81261; 16 = ALHA77081; 17 = Y-8005; 18 = A-881902; see Table 2 for sample classification.

3.3. Reduction State

Reduction phenomena in meteorites can be due to the presence of graphitic carbon in the pristine material from which primitive achondrites accreted. Two main reduction schemes can be proposed [1]:

(1) $(Mg,Fe)_2SiO_4$ (olivine) + C → $MgSiO_3$ (enstatite) + Fe + CO

(2) $2(Mg,Fe)_2SiO_4$ (olivine) + C → $2MgSiO_3$ (enstatite) + 2Fe + CO_2

As a consequence, mafic minerals (olivine and orthopyroxene) are Fe-depleted. Nevertheless, as the solid-state diffusion rate is higher in olivine than in orthopyroxene [37,38], a more marked depletion will be observed for Fa than for Fs. Therefore, a plot of Fe# of orthopyroxene against Mg# of olivine provides a valuable estimate of the reduction state and of the deviations from the expected reduction trend.

In Figure 7, the results obtained from EMPA data on the samples analyzed are presented and compared with literature data: the more reduced meteorites are located in the bottom right corner, while the less reduced ones are near the top left corner. The "normal" reduction trend is therefore represented by a line of negative slope of about −1.

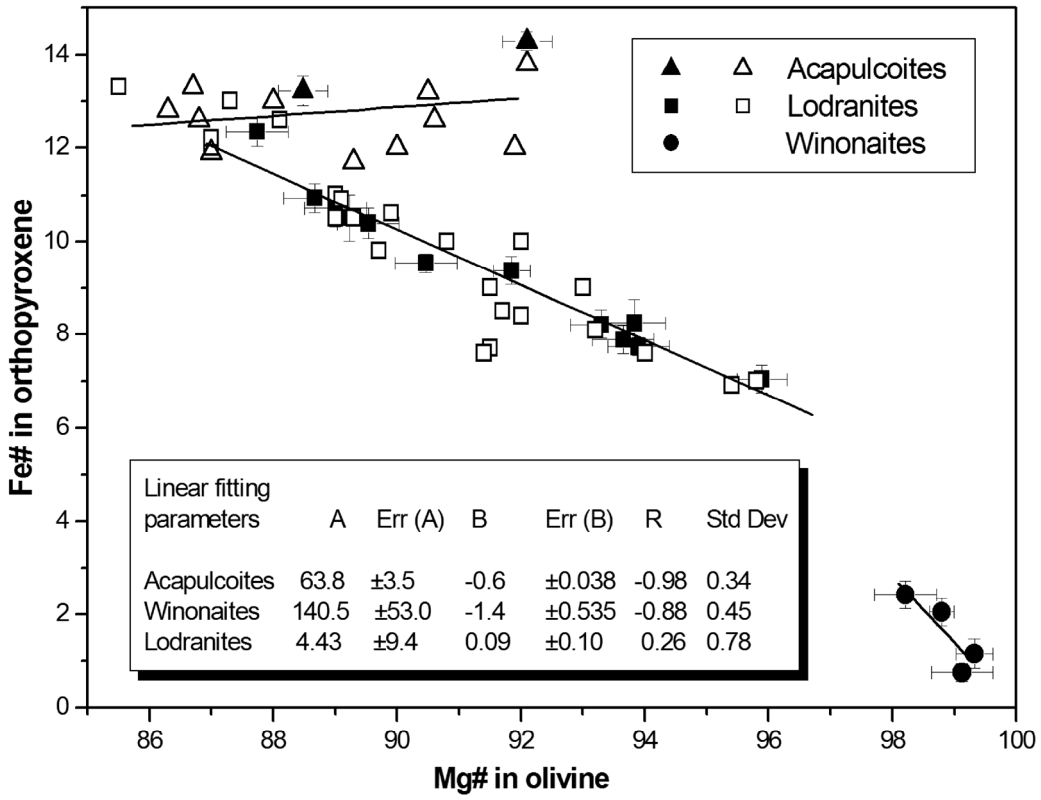

Figure 7. Reduction degree diagram (Fe# in orthopyroxene as a function of the Mg# in olivine) including the linear fitting of the data. Open symbols are literature data [1]. The inset shows the linear fitting parameters for each meteorite group.

It is worth noting that all the acapulcoite and winonaite samples examined in this study agree well with this general trend, *i.e.*, a linear decrease of the Fe# content in orthopyroxene *versus* an increase of the Mg# content for olivine. Conversely, in the lodranite samples, these parameters do not seem to be directly correlated (see Figure 7). Linear fitting of the three separated groups of data suggests the existence of different trends among the primitive achondrites groups: acapulcoites plot along a line

with a slope = −0.6 and are in good agreement with the "normal" reduction process trend described above. Lodranites and winonaites, instead, display a marked deviation from the "normal" trend: lodranites plot mainly in less-reduced portions of the graph, showing almost constant Fe# values with increasing Mg# (dip = +0.09), while winonaites are positioned in the highly-reduced products corner and show a much more steeper slope than acapulcoites (slope = −1.4).

3.4. Metamorphic Temperature

Although primitive achondrites tend to be considered products formed in thermodynamic non-equilibrium conditions, some tentative observations can be forwarded regarding the maximum temperature experimented by these rocks during the metamorphic processes they underwent.

Several geothermometers have been proposed, like the Pt/Pd ratio of troilite [9,39], the Ga, Y, Yb partitioning among clino- and orthopyroxene [40], the olivine-chromite ratio [33] and the two-pyroxene geothermometer, based on the Ca partitioning between ortho- and clinopyroxene in thermodynamic equilibrium conditions.

In order to evaluate the equilibrium temperature experimented by the studied meteorites, we applied the two-pyroxene geothermometer [33]. Accordingly, the studied meteorites experienced temperature values ranging from 900 to 1150 °C. Moreover, a distinctive distribution has been observed: samples belonging to the acapulcoite-lodranite group are divided into two subgroups depending on the presence or absence of chondrules (Figure 8). Chondrule-bearing samples are positioned in the upper-left portion of the diagram, while chondrule-free samples in the lower-right portion. This distribution is in agreement with the hypothesized higher metamorphic degree which may have led to a complete destruction of the chondrules. The exception of the meteorite ALH 81261 may be explained with the low statistic relevance of the chondrule observation, due to the sporadic presence of these relict structures only in selected thin sections of the same meteorite.

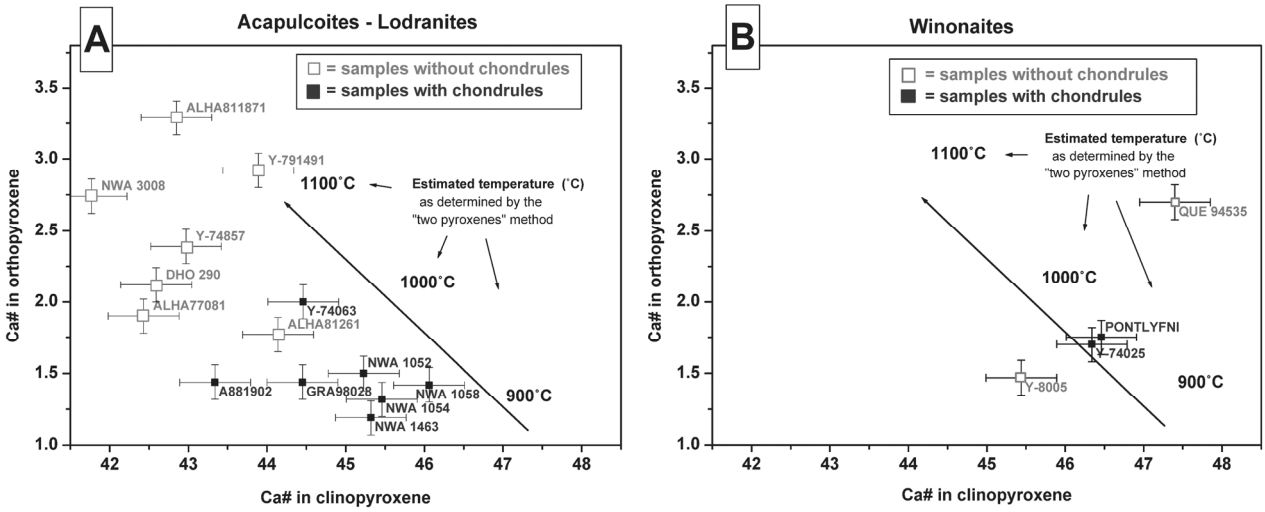

Figure 8. Two pyroxene diagram (Ca content in orthopyroxene as a function of the Ca content in clinopyroxene) for acapulcoites-lodranites (**A**) and winonaites (**B**). Full squares indicate the chondrule-bearing samples, open squares the chondrule-free ones. Superimposed is the line indicating the estimated equilibrium temperature trend as determined by the "two pyroxene" method.

For winonaites no clear trends can be identified. This behavior can be explained by more marked disequilibrium conditions of formation. This assumption is in apparent contrast with the previously cited low compositional variability of olivine. This incongruity can be explained by the different solid-state diffusion rates of olivine compared to pyroxene: a lower homogenization temperature relative to pyroxene is therefore required for olivine. EMPA data, which display a marked compositional homogeneity for olivine and a much higher non-homogeneity for orthopyroxene in winonaites, suggest that these meteorites suffered a petrogenetic process completely different from that of acapulcoite and lodranites.

4. Discussion and Conclusions

A number of considerations can be made regarding the reduction state of primitive achondrites. A possible explanation of the constant Fe# values of lodranites reported in Figure 7 might be that they originate from a chondritic precursor with a reduction state that did not change during metamorphism: in this case, the assumptions described above regarding the olivine-orthopyroxene equilibrium would not be valid. The deviation of the winonaites from the expected "normal" reduction trend can be explained by the existence of a parental body distinct from that of acapulcoites-lodranites, in agreement with previous proposals [8,33,41].

There are many observations in support of this hypothesis:

- The composition of the winonaite parent body might be non-chondritic or, at least, different from that of the presently known classes of chondrites, as the reduction state is intermediate between those of the E and H chondrites [22,42].
- The oxygen isotopic composition is different from that of the acapulcoite-lodranite group [26].
- The high reduction degree might suggest that the parental body of these meteorites formed in an area of the solar system with an oxygen fugacity lower than that of the acapulcoites-lodranites formation area.

An alternative explanation is the existence of a mixing process between primitive materials and more differentiated ones due to asteroidal impacts, with local heating and remixing of fluid and solid phases and, consequently, non-equilibrium cooling [43–47]. This second hypothesis also has experimental support:

- Some samples display an inequigranular texture, with visible shock and rapid cooling features like metal veinlets in silicates.
- Some samples (*i.e.*, Pontlyfni) contain relict chondrules, which is in contrast with the high metamorphic degree required for a marked reduction state.

A possible third explanation considers that they originate from an intrinsically more reduced parent body which was then subjected to impacts, in agreement with [44].

The most common parameter used to distinguish lodranites from acapulcoites and winonaites is based on oxygen isotope measurements [48]. This analysis, although improved and more statistically meaningful than in the past due to the recent discoveries of new samples belonging to these groups, does not take into account the very high textural variability of these samples, especially regarding the presence of pristine material like the chondrules, which is expected to display isotopic features

different from those of the bulk sample. The accurate modal analysis performed using X-ray maps allowed the determination of the modal distribution of the phases of both the chondrules and the matrix in each group of primitive achondrites. Hence, it provides a comprehensive estimate of the silicate/sulfide and mafic/sialic silicate ratios and an accurate evaluation of the metamorphic grade of the studied meteorites and allows their assignment to the acapulcoites or lodranite groups. Moreover, minerochemical parameters such as the Cr and Mn contents of orthopyroxene and the accurate evaluation of the reduction state performed with the Fe# *vs.* Mg# plot, are useful instruments to distinguish winonaites from meteorites belonging to the other groups. Finally, the relationship between the presence of relict chondrules and the metamorphic equilibrium temperature in acapulcoites has been proved for the first time, suggesting the provenance from a different parental body and a different petrogenetic and evolutive history from that of winonaites, for which such a relationship has not been observed. The combined textural and minerochemical investigation has been demonstrated to be a powerful tool in support of oxygen isotopic data offering a more reliable means for the appropriate classification of primitive achondrites.

Acknowledgments

We wish to thank Cecilia Satterwhite of JSC-ARES, Hideyasu Kojima of the AMRC-NIPR, Caroline Smith of the NHM, London, Jochen Schlüter of the Mineralogisches Museum, Universität Hamburg, Alan Rubin of UCLA and Mikhail Nazarov of the Vernadsky Institute for kindly providing some of the meteorite samples studied in this work. This research has been supported with the Royal Astronomical Society 2007 and 2008 grants.

Author Contributions

Vanni Moggi Cecchi and Stefano Caporali performed the experiments; Stefano Caporali analyzed the data; Vanni Moggi Cecchi wrote the paper.

Conflicts of Interest

The authors declare no conflict of interest.

References

1. Rubin, A.E. Petrogenesis of acapulcoites and lodranites: A shock-melting model. *Geochim. Cosmochim. Acta* **2007**, *71*, 2383–2401.
2. Herrin, J.S.; Mittlefehldt, D.W.; Jones, J.H. Early metal records; metal inclusions in acapulcoite-lodranite silicates. In Proceedings of the 68th Annual Meteoritical Society Meeting, Gatlinburg, TN, USA, 12–16 September 2005.
3. McSween, H.Y., Jr. *Meteorites and Their Parent Planets*, 2nd ed.; Cambridge University Press: Cambridge, UK, 1999; p. 324.
4. Mittlefehldt, D.W.; Lindström, M.M.; Bogard, D.D.; Garisson, D.H.; Field, S.W. Acapulco- and Lodran-like achondrites: Petrology, geochemistry, chronology and origin. *Geochim. Cosmochim. Acta* **1996**, *60*, 867–882.

5. Dobrica, E.; Moine, B.N.; Poitrasson, F.; Toplis, M.J.; Bascou, J. Rare earth element insight into the petrologic evolution of the Acapulcoite-Lodranite parent body. In Proceedings of the 39th Lunar and Planetary Science Conference, League City, TX, USA, 10–14 March 2008.
6. Morikawa, N.; Nakamura, N. Silicate melt migration in acapulcoite-lodranite source inferred from alkali and REE abundances (abstract). In Proceedings of the 60th Annual Meteoritical Society Meeting, Maui, HI, USA, 21–25 July 1997.
7. Rubin, A.E. Shock features in acapulcoites and lodranites: Implications for the origin of primitive achondrites. In Proceedings of the 37th Lunar and Planetary Science Conference, League City, TX, USA, 13–17 March 2006.
8. Floss, C. Complexities on the acapulcoite-lodranite parent body: Evidence from trace element distributions in silicate minerals. *Meteorit. Planet. Sci.* **2000**, *35*, 1073–1085.
9. Herrin, J.S.; Mittlefehldt, D.W.; Humayun, M. Thermal constraints from siderophile trace elements in acapulcoite-lodranite metals. In Proceedings of the 37th Lunar and Planetary Science Conference, League City, TX, USA, 13–17 March 2006.
10. Lee, D.C. ^{182}Hf-^{182}W chronometry and the early evolution history in the acapulcoite-lodranite parent body. *Meteorit. Planet. Sci.* **2008**, *43*, 675–684.
11. Touboul, M.; Kleine, T.; Bourdon, B.; van Orman, J.A.; Maden, C.; Zipfel, J. Hf–W thermochronometry: II. Accretion and thermal history of the acapulcoite–lodranite parent body. *Earth Planet. Sci. Lett.* **2009**, *284*, 168–178.
12. Crowther, S.A.; Whitby, J.A.; Busfield, A.; Holland, G.; Busemann, H.; Gilmour, J.D. Collisional modification of the acapulcoite/lodranite parent body revealed by the iodine-xenon system in lodranites. *Meteorit. Planet. Sci.* **2009**, *44*, 1151–1159.
13. McCoy, T.J.; Keil, K.; Clayton, R.N.; Mayeda, T.K.; Bogard, D.D.; Garrison, D.H.; Wieler, R. A petrologic and isotopic study of lodranites: Evidence for early formation as partial melt residues from heterogeneous precursors. *Geochim. Cosmochim. Acta* **1997**, *61*, 623–637.
14. McCoy, T.J.; Keil, K.; Muenow, D.W.; Wilson, L. Partial melting and melt migration in the acapulcoite-lodranite parent body. *Geochim. Cosmochim. Acta* **1997**, *61*, 639–650.
15. Floss, C. LEW 86220: Evidence for melt migration on the acapulcoite-lodranite parent body. In Proceedings of the 31st Lunar and Planetary Science Conference, Houston, TX, USA, 13–17 March 2000.
16. Takeda, H.; Mori, H.; Hiroi, T.; Saito, J. Mineralogy of new Antarctic achondrites with affinity to Lodran and a model of their evolution in an asteroid. *Meteoritics* **1994**, *29*, 830–842.
17. Patzer, A.; Hill, D.H.; Boynton, W.V. Evolution and classification of acapulcoites and lodranites from a chemical point of view. *Meteorit. Planet. Sci.* **2004**, *39*, 61–85.
18. Patzer, A.; Hill, D.H.; Boynton, W.V. An extended classification scheme for the acapulcoites and lodranites. In Proceedings of the 34th Lunar and Planetary Science Conference, League City, TX, USA, 17–21 March 2003.
19. Hidaka, Y.; Yamaguchi, A.; Shirai N.; Sekimoto, S.; Ebihara, M. Lithophile element characteristics of Acapulcoite-Lodranite and Winonaites: Implications for the chemical composition of their precursor materials. In Proceedings of the 43rd Lunar and Planetary Science Conference, The Woodlands, TX, USA, 19–23 March 2012.

20. Hunt, A.C.; Benedix, G.K.; Kreissig, K.; Hammond, S.; Strekopytov, S.; Rehkamper, M. Using geochemical data to assess the evolution of the Winonaite-IAB parent body. In Proceedings of the 43rd Lunar and Planetary Science Conference, The Woodlands, TX, USA, 19–23 March 2012.
21. Davis, A.M.; Ganapathy, R.; Grossman, L. Pontlyfni—A differentiated meteorite related to the group IAB irons. *Earth Planet. Sci. Lett.* **1977**, *35*, 19–24.
22. Benedix, G.K.; McCoy, T.J.; Keil, K.; Bogard, D.D.; Garrison, D.H. A petrologic and isotopic study of winonaites: Evidence for early partial melting, brecciation, and metamorphism. *Geochim. Cosmochim. Acta* **1998**, *62*, 2535–2553.
23. Benedix, G.K.; McCoy, T.J.; Keil, K.; Love, S.G. A petrologic study of the IAB iron meteorites: Constraints on the formation of the IAB-Winonaite parent body. *Meteorit. Planet. Sci.* **2000**, *35*, 1127–1141.
24. Mittlefehldt, D.W.; McCoy, T.J.; Goodrich, C.A.; Kracher, A. Non-chondritic meteorites from asteroidal bodies. *Rev. Mineral. Geochem.* **1998**, *36*, 4.1–4.195.
25. Schulz, T.; Upadhyay, D.; Münker, C.; Mezger, K. Formation and exposure history of non-magmatic iron meteorites and winonaites: Clues from Sm and W isotopes. *Geochim. Cosmochim. Acta* **2012**, *85*, 200–212.
26. Clayton, R.N.; Mayeda, T.K. Oxygen isotope studies of achondrites. *Geochim. Cosmochim. Acta* **1996**, *60*, 1999–2017.
27. Clayton, R.N.; Mayeda, T.K.; Nagahara, H. Oxygen isotope relationships among primitive achondrites. In Proceedings of the 23rd Lunar and Planetary Science Conference, Houston, TX, USA, 16–20 March 1992; pp. 231–232.
28. Moggi Cecchi, V.; Pratesi, G.; Caporali, S. Petrologic and minerochemical investigation of acapulcoites, winonaites and lodranites: New evidences from image analysis and EMPA data. In Proceedings of the 42nd Lunar and Planetary Science Conference, The Woodlands, TX, USA, 7–11 March 2011.
29. Prinz, M.; Waggoner, D.G.; Hamilton, P.J. Winonaites: A primitive achondritic group related to silicate inclusions in IAB irons. In Proceedings of the 11th Lunar and Planetary Science Conference, Houston, TX, USA, 17–21 March 1980; pp. 902–904.
30. Kimura, M.; Tsuchiyama, A.; Fukuoka, T.; Iimura, Y. Antartic primitive achondrites, Yamato-74025, -75300, and -75305: Their mineralogy, thermal history, and the relevance to winonaites. *Proc. NIPR Symp. Antarct. Meteor.* **1992**, *5*, 165–190.
31. Irving, A.J.; Rumble, D. Oxygen isotopes in brachina, SAH 99555 and NWA 1054. In Proceedings of the 69th Annual Meteoritical Society Meeting, Zürich, Switzerland, 6–11 August 2006.
32. Prinz, M.; Nehru, C.E.; Delaney, J.S.; Weisberg, M. Silicate in IAB and IIICD irons, winonaites, lodranites and Brachina: A primitive and modified-primitive group. In Proceedings of the 14th Lunar and Planetary Science Conference, Houston, TX, USA, 14–18 March 1983; pp. 616–617.
33. Benedix, G.K.; Lauretta, D.S. Thermodynamic constraints on the formation history of acapulcoites. In Proceedings of the 37th Lunar and Planetary Science Conference, League City, TX, USA, 13–17 March 2006.
34. El Goresy, A.; Zinner, E.; Pellas, P.; Caillet, C. A menagerie of graphite morphologies in the Acapulco meteorite with diverse carbon and nitrogen isotopic signatures: Implications for the evolution history of acapulcoite meteorites. *Geochim. Cosmochim. Acta* **2006**, *69*, 4535–4556.

35. Rubin, A.E. Postshock annealing and postannealing shock in equilibrated ordinary chondrites: Implications for the thermal and shock histories of chondritic asteroids 1. *Geochim. Cosmochim. Acta* **2004**, *68*, 673–689.
36. Takeda, H.; Huston, T.J.; Lipschutz, M.E. On the chondrite-achondrite transition: Mineralogy and chemistry of Yamato 74160 (LL7). *Earth Planet. Sci. Lett.* **1984**, *71*, 329–339.
37. Buseck, P.R. Phosphide from meteorites: Barringerite, a new iron-nickel mineral. *Science* **1969**, *165*, 169–171.
38. Holzheid, H.; Palme, H.; Chakraborty, S. The activities of NiO, CoO and FeO in silicate melts. *Chem. Geol.* **1997**, *139*, 21–38.
39. Herrin, J.S.; Mittlefehldt, D.W.; Humayun, M. History of metal veins in acapulcoite-lodranite clan meteorite GRA 95209. In Proceedings of the 69th Annual Meteoritical Society Meeting, Zürich, Switzerland, 6–11 August 2006.
40. Burkhardt, C.; Witt-Eickschen, G.; Palme, H. Thermometry of Landes silicate inclusions and acapulcoites based on *in situ* trace element analyses. In Proceedings of the 69th Annual Meteoritical Society Meeting, Zürich, Switzerland, 6–11 August 2006.
41. Floss, C. Acapulcoite—Lodranite petrogenesis: Clues from trace element distributions in individual minerals. In Proceedings of the 29th Lunar and Planetary Science Conference, Houston, TX, USA, 16–20 March 1998.
42. Airieau, S.A.; Farquhar, J.; Thiemens, M.H.; Leshin, L.A.; Bao, H.; Young, E. Planetesimal sulfate and aqueous alteration in CM and CI carbonaceous chondrites. *Geochim. Cosmochim. Acta* **2005**, *69*, 4167–4172.
43. Choi, B.G.; Ouyang, X.; Wasson, J.T. Classification and origin of IAB and IIICD iron meteorites. *Geochim. Cosmochim. Acta* **1995**, *59*, 593–612.
44. Benedix, G.; Lauretta, D.; McCoy, T. Thermodynamic constraints on the formation conditions of winonaites and silicate-bearing IAB irons. *Geochim. Cosmochim.* **2005**, *69*, 5123–5131.
45. Floss, C. Acapulcoite complexities: Clues from trace element distributions. In Proceedings of the 65th Annual Meteoritical Society Meeting, Los Angeles, CA, USA, 21–26 July 2002.
46. Scott, E.R.D.; Krot, T.V.; Goldstein, J.I.; Benedix, G.K. Thermal and impact histories and origin of Winonaites and IAB iron meteorites. In Proceedings of the 77th Annual Meeting of the Meteoritical Society, Casablanca, Morocco, 8–13 September 2014.
47. Grady, M.; Pratesi, G.; Moggi Cecchi, V. *Atlas of Meteorites*, 1st ed.; Cambridge University Press: Cambridge, UK, 2014; p. 314.
48. Greenwood, R.C.; Franchi, I.A.; Gibson, J.M.; Benedix, G.K. Oxygen isotope variation in primitive achondrites: The influence of primordial, asteroidal and terrestrial processes. *Geochim. Cosmochim. Acta* **2012**, *94*, 146–163.